Journal of Nano- and Electronic Physics
Vol. **17** No 2, 02030(5pp) (2025)

Журнал нано- та електронної фізики
Том **17** № 2, 02030(5cc) (2025)

OPEN ACCESS

REGULAR ARTICLE

Spintronic Prospects of Half-Heusler Alloy MnAuSn: DFT and Hybrid Functional Studies of Magnetic and Electronic Properties

N. Bouteldja[1,*], I. Ouadha[2,†], M. Traiche[1,‡], S. Dahmane[1,§], H. Rached[2,**], M.H. Meliani[1,††]

[1] *Theoretical Physics and Materials Physics Laboratory, Hassiba Benbouali University, Chlef, Algeria*
[2] *Magnetic Materials Laboratory, Djillali Liabes University, Sidi Bel-Abbes, Algeria*

(Received 22 November 2024; revised manuscript received 23 April 2025; published online 28 April 2025)

In this study, we use the full potential linearized augmented plane wave (FP-LAPW) method within the framework of density functional theory combined with ab-initio calculations with hybrid exchange-correlation functional to determine the structure and investigate the electronic and magnetic properties of zinc-blende MnAuSn alloy. The magnetic state is confirmed to be the most stable configuration using the Perdew-Burke-Ernzerhof (PBE) generalized gradient approximation (GGA). Our spin-polarized band structure simulations indicate that the material exhibits half-metallic behavior. The complex interplay affecting the magnetic and electronic properties is mainly attributed to the hybridization between the Mn-d, Au-f and Sn-p states, which leads to the observed spin polarization. MnAuSn shows traits of a half-metallic ferromagnet, as evidenced by a calculated total magnetic moment of 4 μB. Grasping these properties is crucial for leveraging the unique features of these material in future technological applications, such as spintronic devices.

Keywords: Spintronic, PBE+H, HHA, MnAuSn, Half-Metal, Magnetic material.

DOI: 10.21272/jnep.17(2).02030 PACS numbers: 85.75. – d, 75.50. – y, 71.15.Mb

1. INTRODUCTION

Studies of HHA such as MnAuSn have highlighted their exceptional electronic and thermoelectric properties, making them ideal candidates for next-generation technologies. Studies have shown that external factors such as stress can induce electronic phase transitions in AuMnSn, improving its suitability for tunable systems [2,3]. Additionally, the importance of localized Mn moments in Mn-based HHA has been emphasized, broadening their potential for transport applications [4].

Experimental work has further explored the structural and electronic behavior of MnAuSn. Optical studies have revealed the role of Sn sites in contributing to the magneto-optical Kerr effect, a critical characteristic for optical applications [5]. Moreover, thermoelectric properties have been extensively studied, with AuMnSn recognized as a promising material for energy conversion technologies [6,7].

Discrepancies between experimental and theoretical measurements, particularly in the Kerr effect, have led to refinements in modeling techniques [8]. Predictions of significant Kerr rotation in related alloys suggest that doping could expand their potential applications [9,10].

The advancements in HHA are rooted in their high Curie temperatures and tunable properties, enabling versatile applications [11-13]. Their operational advantages make them ideal for diverse uses. Ground states and electronic behaviors in related systems have been extensively studied, aiding in their characterization.

This study investigates the role of exchange-correlation potential in shaping the electronic structure and magnetic properties of the Half-Heusler MnAuSn Alloy. Spin-polarized band structure analysis was conducted using the PBE with an onsite Hybrid exchange–correlation treatment, which provided additional insights into gradient-corrected electronic interactions, demonstrating the complementary strengths of PBE+H in understanding and predicting the behavior of HHA.

2. CALCULATION DETAILS

The calculations in this study were performed using the Full Potential Linear Augmented Plane Wave (FP-LAPW) method using the WIEN2k software package [14,15]. Spin polarization calculations were performed using the PBE+H method [16] as described by Moreira et al. [17]:

* Correspondence e-mail: n.bouteldja@univ-chlef.dz
† i.oudha@univ-chlef.dz
‡ md.traiche@univ-chlef.dz
§ s.dahmane@univ-chlef.dz
** h.rached@univ-chlef.dz
†† m.hadjmeliani@univ-chlef.dz

Cite this article as: N. Bouteldja et al., *J. Nano- Electron. Phys.* 17 No 2, 02030 (2025) https://doi.org/10.21272/jnep.17(2).02030

$$E_{XC}^{PBE+H} = E_{XC}^{PBE} + \alpha\left(E_X^{HF} + E_X^{PBE}\right) \quad (1)$$

Where (α) signifies the fraction of Hartree-Fock (HF) exchange. In this work, we used the default value of (0.25). The wave functions and potentials were expanded using a muffin-tin approach for atomic sites and plane waves in the interstitial region. The cutoff parameters included: Muffin-tin sphere cutoff ($I_{max} = 10$), interstitial region cutoff ($R_{min} = 8$) and Energy cutoff from valence to core states (10^{-3}Ryd) to distinguish. A dense k-point network of 1000 points was used to sample the first Brillouin zone, ensuring convergence and accuracy in the calculations of energy, magnetic moments and spin polarization. The atomic positions in the MnAuSn unit cell were defined as follows: Mn at 4*a* (0, 0, 0), Au at 4*b* (1/4, 1/4, 1/4) and Sn at 4*c* (1/2, 1/2, 1/2). Muffin-tin Radii (R_{mt}) were selected as 2.1 for Sn, 2.4 for Mn and Au.

3. RESULTS AND DESCUSSION

3.1 Ground Magnetic State

The total energy was optimized by adjusting the supercell volume using the Two-Dimensional Optimize package [18]. The equilibrium structural parameters were obtained by minimizing the total energy as a function of unit cell volume at $T = 0$ K. This optimization was performed using Murnaghan equation of state [19], which provides an accurate fit for the relationship between total energy and primitive cell volume:

$$E(V) = E_0 + \frac{B}{B'(B'+1)}\left[V\left(\frac{V_0}{V}\right)^{B'} - V_0\right] + \frac{B}{B'} + (V-1) \quad (2)$$

In this equation, the bulk modulus (B), its pressure derivative (B') and equilibrium volume (V_0) were extracted from these calculations. The bulk modulus B is derived from the relationship:

$$B = V\frac{\partial^2 E}{\partial V^2} \quad (3)$$

Fig. 1 demonstrates two types of electronic configurations: non-spin-polarized and spin-polarized. The most stable phase of MnAuSn corresponds to the magnetic state, suggests that the spin-polarized configuration lowers the system energy, stabilizing the MnAuSn. This implies that the electron spin ordering plays a crucial role in determining the material overall energy and stability. The magnetic state refers to a configuration where the material exhibits a non-zero magnetic moment, meaning the electron spins are aligned in a way that creates a net magnetic effect.

The structural parameters of MnAuSn such as the lattice parameter (L_P), the compressibility modulus (B, B') and the minimum energy obtained from the calculations are presented in Table 1.

3.2 Band Structure

Fig. 2 shows the spin-polarized electronic band structure in the first Brillouin zone, calculated along the symmetry directions for MnAuSn. It reveals an indirect energy gap of 0.275 eV in the spin-down configuration, occurring between the top of the valence band at the Γ point and the bottom of the conduction band at the X point, which demonstrates semiconductor character. In contrast, the spin-up configuration exhibits an overlap between the bands and the Fermi level (E_F) indicating metallic character. The band structure of MnAuSn with spin-polarization (spin-up and spin-down) is not identical, confirming that the MnAuSn compound exhibits half-metallic behavior.

3.3 Density of State

Fig. 3 depicts the Spin-dependent Total Density of States (STDOS) for MnAuSn, shown the origin of states and bands in MnAuSn. The bands near the Fermi level primarily arise from from the Mn atom withontributions from the Au atom and a minor influence from the Sn atom. At Fermi level, the Mn atom strongly impacts the magnetic properties, while Au and Sn atoms alter the electronic environment through their interactions with Mn. The spin asymmetry at the Fermi level reveals pronounced spin polarization, which underlies the half-metallic behavior and contributes to the net magnetic moment.

The Spin-dependent Partial Density of States (SPDOS) showed in Figs. 4, 5 and 6 for Mn, Au and Sn respectively, reveal distinct contributions from their electronic states. The PDOS of Mn is primarily derived from the 3d states, which influence the magnetic properties. The PDOS of Au is dominated by the 4f states, which are crucial for the alloy electronic structure. Finally, the PDOS of Sn mainly originates from the 5p states, contributing to the material bonding and electronic interactions.

Table 1 – Structural properties of MnAuSn calculated for PBE + H in comparison with the experimental and other theoretical data

Parameter	PBE+H		PBE+U [2]	PBE [2]	Other works	Exp
	Non-magnetic	Magnetic				
LP (A°)	6.05247	6.14802	6.2194 6.3263	6.2125 6.2252	6.197 [25] 6.3233 [26]	6.338 [20,21,22] 6.323 [23,24]
B (GPa)	84.7721	88.9613	84.60 86.94	86.43 85.26	85.3 [27]	/
B'	5	5	5.0188 5.0681	5.0265 5.1058	/	/
Emin (Ry)	– 52771.22492	– 52771.32537	/	/	/	/

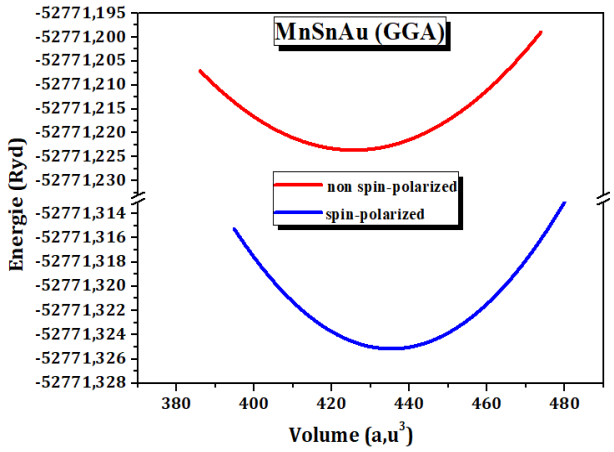

Fig. 1 – Energy versus volume of MnAuSn with PBE+H calculation

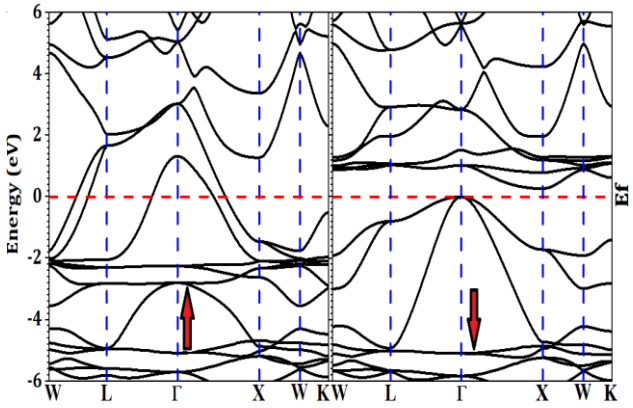

Fig. 2 – Spin-polarized band structure of MnAuSn with PBE+H calculation

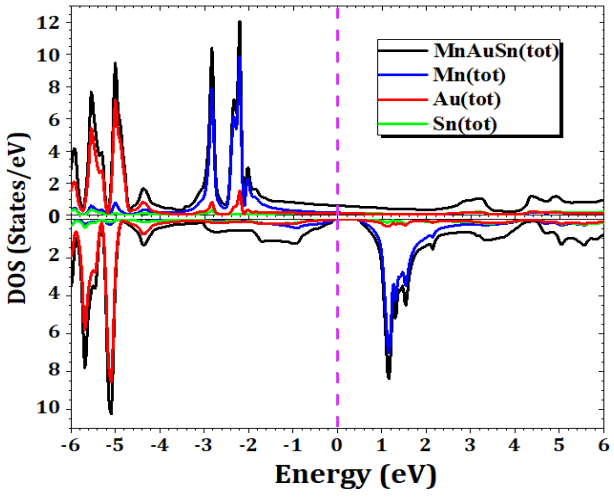

Fig. 3 – Spin-dependent total of MnAuSn with PBE+H calculation

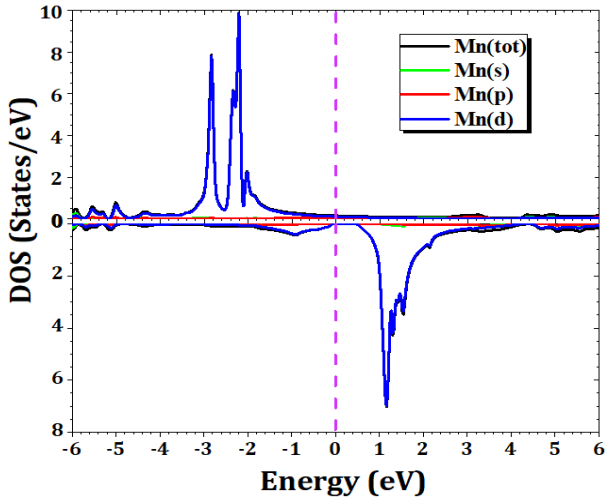

Fig. 4 – Spin-dependent partial of Mn with PBE+H calculation

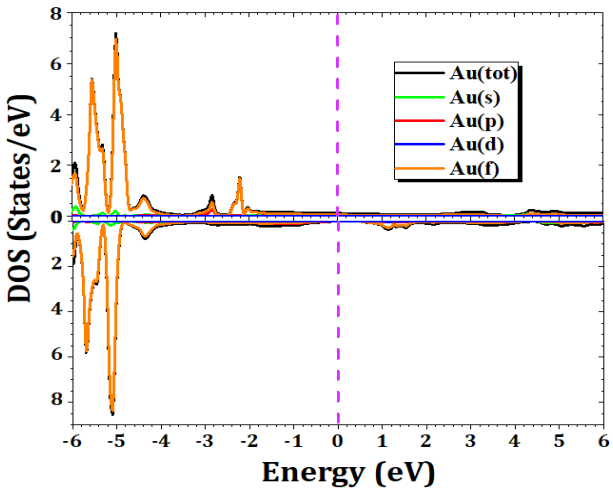

Fig. 5 – Spin-dependent partial of Au with PBE+H calculation

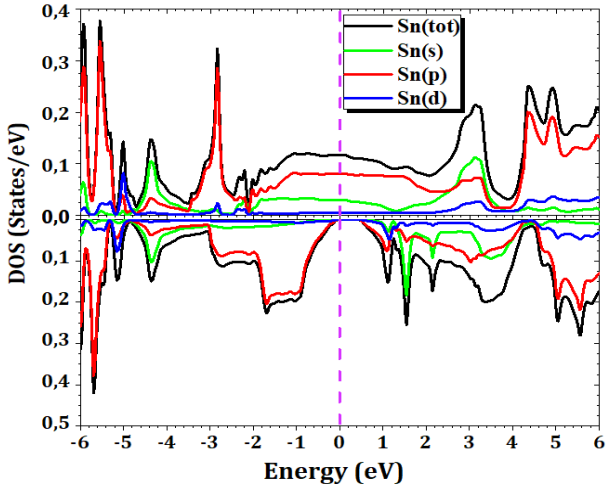

Fig. 6 – Spin-dependent partial of Au with PBE+H calculation

The primary mechanism behind this spin polarization is the spd-hybridization of Mn-d, Au-f and Sn-p states. This hybridization not only results in the observed spin polarization but is also the main driver of the material half-metallic nature. Furthermore, the partial occupancy of the spin-down states at the Fermi level gives rise to the net magnetic moment in MnAuSn, highlighting the importance of hybridization in determining its electronic and magnetic behavior.

3.4 Magnetic Moment

In its free state, Mn typically exhibits a local magnetic moment of 5 μB due to unpaired 3d-electrons, while Sn and Au are non-magnetic as their 4d and 4f electrons are paired. In the MnAuSn compound, Mn interacts with Sn and Au atoms, leading to hybridization between Mn-d electrons, Sn-p electrons and Au-f electrons. This results in a redistribution of charge density and reduces Mn magnetic moment to 4 μB. The delocalization of Mn-d electrons weakens its magnetic contribution, affecting the stability of hybridized states. These inter-atomic interactions are crucial for the magnetic properties of MnAuSn, which are important for spintronic applications. Additionally, the local magnetic moment of Sn is negative, indicating anti-parallel alignment with Mn, while Au shows a positive value, indicating parallel alignment, as shown in Table 2.

Table 2 – Calculated total, local and interstitial magnetics moments of MnAuSn

Magnetic Moments	This Work	Other Works [2]	
	PBE+H	PBE+U	PBE
Mint (μB)	0.08182	/	/
MMn (μB)	3.91332	3.426	3.363
MAu (μB)	0.04121	0.07	0.073
MSn (μB)	-0.03778	-0.155	-0.144
Mtot (μB)	3.99857	3.34 3.724	3.292 3.71

4. CONCLUSION

MnAuSn Half-Heusler Alloy studied using PBE+H for correlated systems, exhibits half-metallic behavior with a reduced local magnetic moment of Mn (4 μB) due to the hybridization between Mn-3d, Sn-4p and Au-4f electrons. This hybridization weakens Mn magnetic contribution and highlights the role of inter-atomic interactions in determining the alloy magnetic properties. The local magnetic moments of Sn and Au atoms align anti-parallel and parallel to Mn, respectively. These findings are important for designing materials with tailored magnetic properties for spintronic applications.

REFERENCES

1. J. Kawasaki, S. Chatterjee, P. Canfield, *MRS Bull.* **47**, 555 (2022).
2. A. Amudhavalli, R. Rajeswarapalanichamy, K. Iyakutti, *J. Alloy. Compd.* **708**, 1216 (2017).
3. L. Offernes, A. Torgersen, A. Kjekshus, *J. Alloy. Compd.* **307**, 174 (2000).
4. J. Karel, F. Bernardi, C. Wang, R. Stinshoff, N. Born, S. Ouardi, U. Burkhardt, G. Fecher, C. Felser, *Phys. Chem. Chem. Phys.* **17** No 47, 31707 (2015).
5. X. Shang, Y. Wang, M. Tan, *Adv. Mater. Res.* **750-752**, 941 (2013).
6. K. Xia, C. Hu, C. Fu, X. Zhao, T. Zhu, *Appl. Phys. Lett.* **118**, 140503 (2021).
7. G. Rogl, P. Rogl, *Crystals* **13** No 7, 1152 (2023).
8. P. Ravindran, L. Offernes, A. Kjekshus, *Appl. Phys. Lett.* **91**, 216101 (2007).
9. S. Lee, Y. Janssen, J. Park, B. Cho, *Appl. Phys. Lett.* **88**, 121909 (2006).
10. L. Offernes, P. Ravindran, A. Kjekshus, *Appl. Phys. Lett.* **82**, 2862 (2003).
11. K. Elphick, W. Frost, M. Samiepour, T. Kubota, K. Takanashi, H. Sukegawa, S. Mitani, A. Hirohata, *Sci. Technol. Adv. Mater.* **22**, 235 (2020).
12. F. Casper, V. Ksenofontov, H. Kandpal, S. Reiman, T. Shishido, M. Takahashi, M. Takeda, C. Felser, *Zeitschrift für anorganische und allgemeine Chemie* **632**, 1273 (2006).
13. A. Neumann, L. Offernes, A. Kjekshus, B. Klewe, *J. Alloy. Compd.* **274**, 136 (1998).
14. P. Blaha, K. Schwarz, G.K.H. Madsen, D. Kvasnicka, J. Luitz, *An Augmented Plane Wave Plus Local Orbitals Program for Calculating Crystal Properties* (Ed. by K. Schwarz) (Techn. Universität Wien, Austria: 2001).
15. F. Tran, P. Blaha, K. Schwarz, P. Novák, *Phys. Rev. B* **74** No 15, 155108 (2006).
16. J.P. Perdew, K. Burke, M. Ernzerhof, *Am. Phys. Soc.* **77** No 18, 3865 (1996).
17. I. de P.R. Moreira, F. Illas, R.L. Martin, *Phys. Rev. B* **65**, 155102 (2002).
18. A.H. Reshak, M. Jamal, *J. Alloy. Compd.* **555**, 362 (2013).
19. F.D. Murnaghan, *Proc. Nat. Acad. Sci.* **30** No 9, 244 (1944).
20. A. Neumann, A. Kjekshus, C. Rømming, E. Røst, *J. Alloy. Compd.* **240**, 42 (1996).
21. L. Offernes, A. Torgersen, H. Brinks, A. Kjekshus, B. Hauback, *J. Alloy. Compd.* **288**, 117 (1999).
22. L. Offernes, P. Ravindran, A. Kjekshus, *J. Alloy. Compd.* **439**, 37 (2007).
23. J.S. Kang, J.H. Hong, S.W. Jung, Y.P. Lee, J.G. Park, C.G. Olson, S.J. Youn, B.I. Min, *Solid State Commun.* **88**, 653 (1993).
24. X. Shang, Y. Wang, M. Tan, *Adv. Mater. Res.* **750**, 941 (2013).
25. M. Amft, P.M. Oppeneer, *J. Phys. Condens. Matter* **19**, 315216 (2007).
26. A. Neumann, L. Offernes, A. Kjekshus, B. Klewe, *J. Alloy. Compd.* **274**, 136 (1998).
27. T. Chibueze, A. Raji, C. Okoye, *J. Phys. Chem. Solid.* **139**, 109328 (2020).

Перспективи спінтроніки на основі напівгейслерового сплаву MnAuSn: дослідження магнітних та електронних властивостей за допомогою DFT і гібридних функціоналів

N. Bouteldja[1], I. Ouadha[2], M. Traiche[1], S. Dahmane[1], H. Rached[2], M.H. Meliani[1]

[1] *Theoretical Physics and Materials Physics Laboratory, Hassiba Benbouali University, Chlef, Algeria*
[2] *Magnetic Materials Laboratory, Djillali Liabes University, Sidi Bel-Abbes, Algeria*

У даному дослідженні застосовано метод повного потенціалу з лінеаризованими розширеними хвильовими функціями (FP-LAPW) в рамках теорії функціонала густини (DFT) у поєднанні з гібридним обмінно-кореляційним функціоналом для визначення структури та вивчення електронних і магнітних властивостей сплаву MnAuSn з кристалічною структурою типу цинкової обманки (zinc-blende). Магнітна конфігурація підтверджена як найстабільніший стан при використанні узагальненого градієнтного наближення Пердью–Берк–Ернзергофа (PBE-GGA). Результати спін-залежних розрахунків зонної структури вказують, що даний матеріал має напівметалічну поведінку. Складна взаємодія, що визначає магнітні та електронні характеристики, головним чином пов'язана з гібридизацією станів Mn-3d, Au-4f та Sn-5p, що й забезпечує спінову поляризацію. Матеріал MnAuSn демонструє властивості напівметалічного феромагнетика, що підтверджується розрахованим загальним магнітним моментом 4 μB. Розуміння таких властивостей є важливим для використання у спінтроніці та розробки новітніх електронних пристроїв, які ґрунтуються на маніпулюванні спіном електрона.

Ключові слова: Спінтроніка, PBE+H, Напівгейслерові сплави, MnAuSn, Напівметал, Магнітний матеріал.